Annex S – CM LABS FINAL REPORT

Note: This Annex appears in its original format.

NORTH ATLANTIC TREATY ORGANIZATION

RESEARCH AND TECHNOLOGY ORGANIZATION

AC/323()

www.STO.nato.int

STO TECHNICAL REPORT

CM Labs AVT-248 NG-NRMM Final Report

Final report describing the modelling efforts carried out by CM Labs on the FED Alpha, and comparison to vehicle test results

Table of Contents

List of Figures

LIST OF FIGURES

LIST OF TABLES

Chapter 1 – Project Description

This document describes benchmarks produced by CM-Labs Simulations Inc (CML). to address the NATO committee led by TARDEC (AVT-248) for the development of a Next Generation NATO Reference Mobility Model. CM-Labs has modeled the FED Alpha vehicle from the available data and performed the required tests. A high level overview of the results as compared to actual test results collected at the Keewanaw Research Center (KRC), along with some discussion are included in this document.

Chapter 2 – Vehicle Model and Assumptions

The vehicle was modelled as closely as possible according to the provided specifications and discussions, but some assumptions and simplifications had to be made in certain cases. The following outlines some of the model details that warrant explanation. Assumption relating to specific tests are listed in the chapters corresponding to the tests.

GENERAL

- All modelling was done using CM Labs Simulations' Vortex Studio software. Vortex Studio is a unified simulation and visualisation platform that allows you to create true-to-life simulations of land and sea equipment and environments, or integrate its components into other software. Vortex is also used in hardware in the loop simulations for design purposes.
- Vortex Studio provides an efficient multi-body solver, with modules for modelling vehicles, earth moving and construction machines.
- The modelling was performed on an internal development branch of Vortex that will soon be released as Vortex Studio 2019A.
- The simulation time step was set to 10 milliseconds (100 Hz) for all tests except Ride Quality, which was simulated with a time step of 2.5 ms (400 Hz).

CHASSIS AND SUSPENSION

- While the centre of gravity of the chassis was provided, the x and y locations were modified to match weight distribution provided by KRC measurements.
- All components of the suspension and steering system that had positions and mass properties provided were modelled.
- Compliance in the control arm bushings was modelled according to provided stiffness and damping.
- Compliance in the steering system and behaviour of the power assist system was not modelled, since information was not available. All steering control was performed directly on the pitman arm.
- The Koni Frequency Selective Damper (FSD) was modelled according to the provided model, but the actual behaviour of the suspension seemed to deviate from the provided model, particularly for the half-round tests. In order to improve this performance, the low and high frequency curves of the FSD model were modified to closer match the calibration test results. It is not surprising that the damper behaviour after several years in storage and many high-impact tests would be different from initially designed.
- The suspension air bag inflation system was modelled and set corresponding to the high ride height.
- Aerodynamic drag was applied, assuming a drag coefficient times front area (CdA) of 2.28.

DRIVE TRAIN

- In order to account for drive train efficiency and losses due to fans and auxiliary loads and the fact that the engine is limited to 90% output, the net torque provided by the engine reduced from the provided engine torque data.

- Additional losses were added to the system to account for inefficiencies in the drive shafts, transmission, and differentials.
- Transmission and differential gear ratios were modelled according to provided data.
- The transmission shifting schedule and torque converter lockup was tuned to match provided data and calibration tests.
- Details about transmission clutching and shifting behaviour were not provided so this was tuned according to acceleration calibration test data. Currently, the shift lasts 0.8 seconds, and throttle is partly lifted during this period.

TIRE AND HARD GROUND MODELLING

- The tire stiffness was modelled according to the provided data at 35 psi, and damping was assumed to be low (1% of stiffness).
- Pavement terrain was considered non-compliant.
- Gravel terrains have a small compliance, but it is small compared to tire compliance.
- Rolling resistance of 1.5% was applied.
- The Pacejka Magic Formula 2002 model (defined in 2002) was used for all tests on pavement, using parameters provided.
- Gravel tests used a Coulomb friction model where the friction force is equal to or less than the normal force multiplied by the coefficient of friction. The coefficient itself was defined by KRC Saab friction tests. The following parameters were used:

Table 1: Gravel friction coefficients

Gravel Type	Coefficient of Friction
Compacted Gravel	0.37
Compacted Crushed Rock	0.44
Rink Stability Compact	0.50

SOFT SOIL MODELLING

The soft ground modelling in Vortex Studio is based on the Bekker/Wong/Janosi/Hanamoto (BWJH) model. It is based on the parametric analysis of wheel-soil interaction was proposed by Bekker [3]. This model and its extension proposed by Wong and Reece [6] are widely used, as they have been experimentally validated and are computationally efficient. Other variations exist.

The BWJH model employs a pressure-sinkage relationship proposed by Bekker [4] for representation of the normal stress. The longitudinal shear stress is expressed using a formulation from Janosi and Hanamoto [5]. Details

of the expressions can be found in [7] and a discussion of this and other semi-empirical terramechanics models is provided in [1].

The BWJH model had already been implemented in Vortex. For implementation details of the model, and specifically how to make the constitutive terramechanics equations compatible with real-time multi-body dynamics simulation and transient motion states, please refer to [2].

Many sets of model parameters based on KRC measurements were tested, but eventually a single set was chosen for each of six different soil types used in the testing events, which can be seen in Table 2**Error! Reference source not found.**.

Table 2: Properties for soft soil used in BWJH model and corresponding references.

Type	N	Kc	Kphi	K int	C int	Phi int	K ext	C ext	Phi ext
		kN/m^(n+1)	kN/m^(n+2)	cm	kPa	Degrees	cm	kPa	Degrees
2NS	0.51	56.15	410	2.14	1.35	31.99	0.88	0.02	26.75
FGD	1.74	0.00	318069	1.89	1.25	36.66	0.76	0.00	28.77
FGW	4.03	0.00	4378384	3.01	3.63	35.17	0.68	0.43	28.80
CGD	0.63	74.01	1087	2.16	1.34	31.35	0.95	0.14	26.70
RN	2.27	0.00	5848191	0.91	1.72	39.59	0.70	0.11	31.76
STB	2.82	480643.15	1190520	1.67	3.34	39.60	0.51	0.28	34.12

In cases where Kc is zero, an alternative pressure sinkage was used, which depends only on Kphi. Three parameters (K, c, and phi) have different parameters for internal slip between the soil and itself (int) and external slip between soil and rubber (ext).

Descriptions of the parameters can be seen in Table 3, and a detailed explanation of the model parameters can be found in [7].

Table 3: Parameter definitions for BWJH model

Parameter	Description	Units
n	Sinkage exponent	-
Kc	Pressure-sinkage module	$\mathrm{kN/m}^{n+1}$
Kphi	Pressure-sinkage module	$\mathrm{kN/m}^{n+2}$
K	Longitudinal soil deformation module	cm
c	Soil cohesion	kPa
phi	Soil internal friction angle	°

Based on provided information, the ratio of lug to overall contact area is 63.2%.

Chapter 3 – Test 1: Straight Line Acceleration

In this test, the vehicle was accelerated at full throttle and allowed to shift automatically for until maximum speed was reached.

ASSUMPTIONS

- This test was performed on pavement.

RESULTS

The following plots show the results from running an acceleration test, compared to KRC test results.

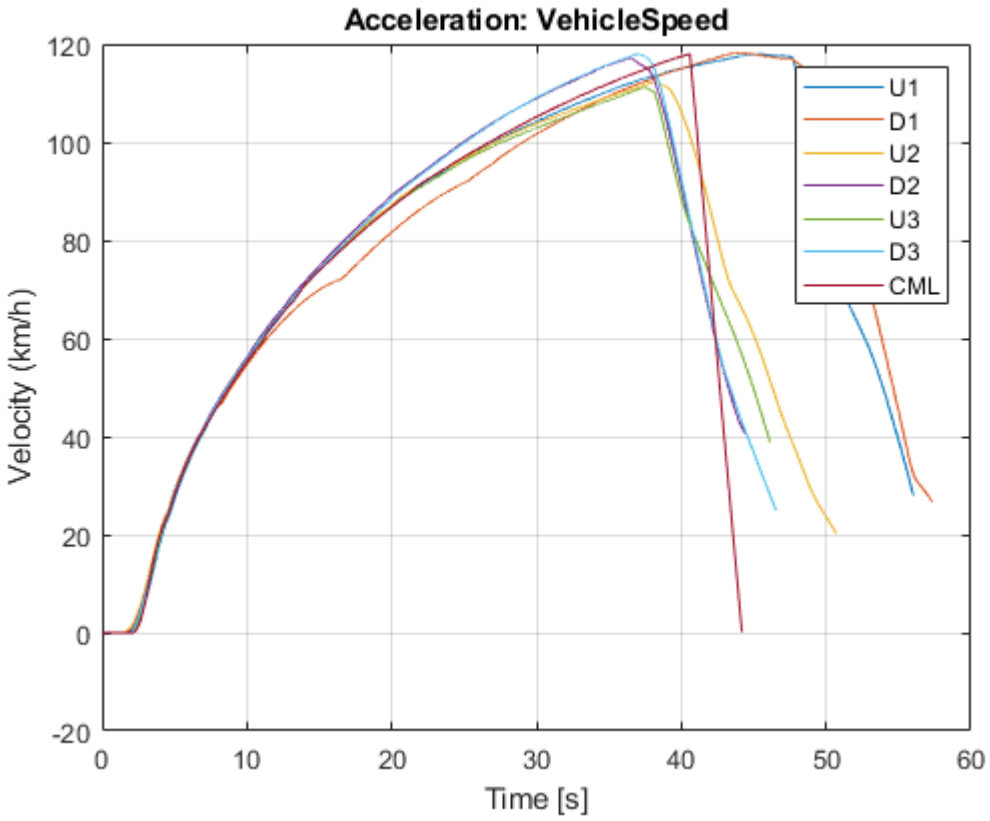

Figure 1: CML simulation vehicle speed, compared to six KRC test results, for uphill and downhill paths

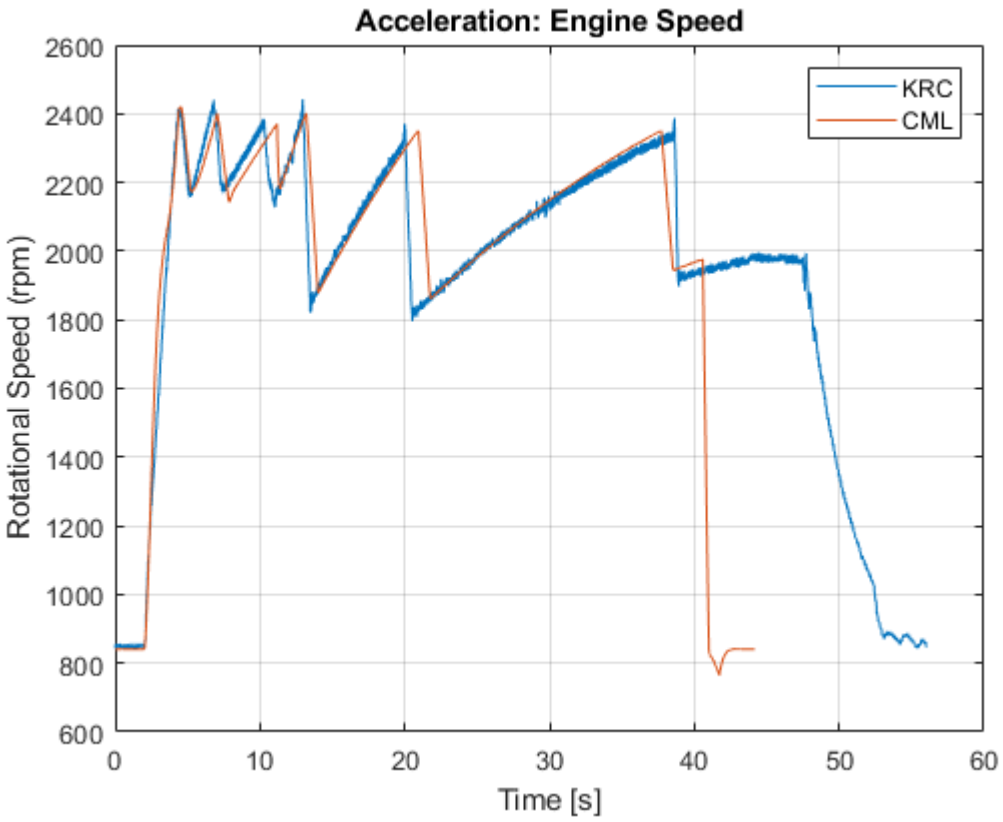

Figure 2: Engine RPM compared between CML and KRC test results

COMMENTS AND CONCLUSIONS

The simulation speed plot (Figure 1) almost precisely matches the average of the test speed plots. As the test plots are performed in two directions to compensate for slope and wind, the average is exactly what the test plot should match.

Figure 2 shows the RPM range and shifting points also match very well, including the torque converter lock-up, which appears like a shifting point at about 10 seconds.

Chapter 4 – Test 2: Wall to Wall Turn Circle

In this test, the vehicle was driven slowly in a circle at maximum steering.

ASSUMPTIONS

- This test was performed on pavement.
- The vehicle was moving at about 2 km/h.

RESULTS

The positions of the front left and front right corners of the vehicle were plotted while the vehicle was driven clockwise (CW) for one circle, then counter-clockwise (CCW).

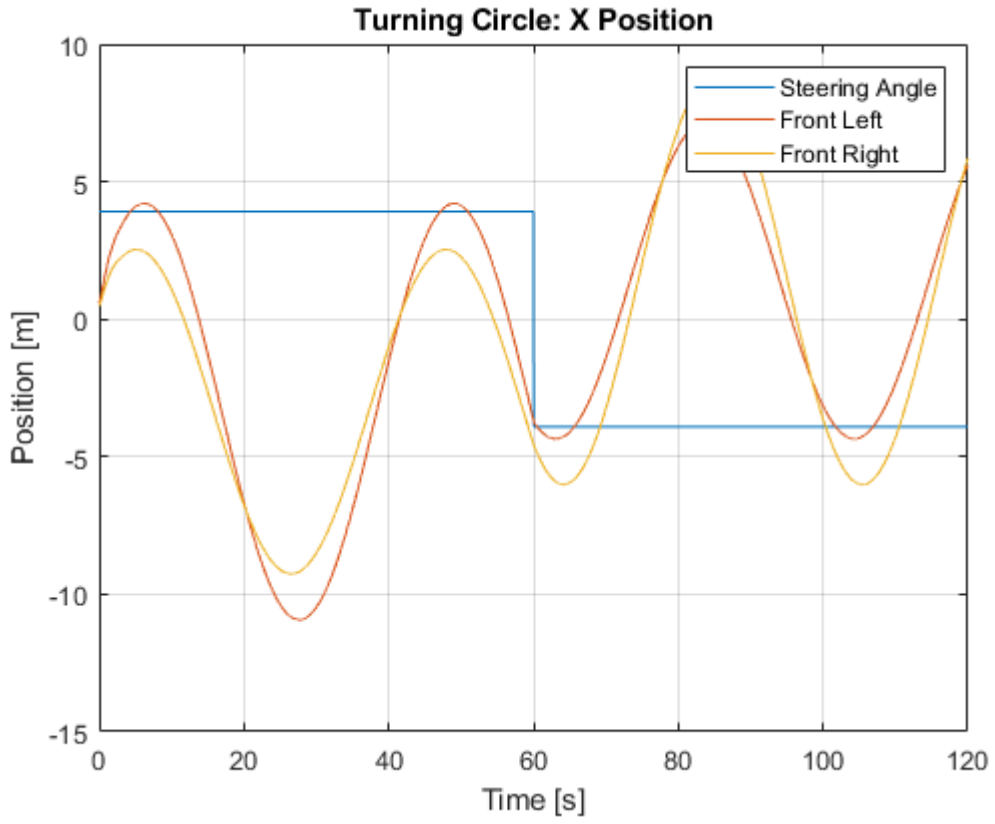

Figure 3: Steering input and vehicle corner positions for turning circle

By measuring the difference from the minimum and maximum positions of the front left corner for the CW and front right corner for CCW, the minimum turning circle can be determined and compared to the vehicle test results.

Table 4: Minimum turning diameter

	CW (m)	CCW (m)
KRC Test	15.6	15.5
Simulation	15.1	14.8

COMMENTS AND CONCLUSIONS

The simulated turning circle is reasonably close to the KRC test results, indicating the steering system linkages and pitman arm range are accurate.

Chapter 5 – Test 3: Steady State Cornering

In this test, the vehicle was driven around a circle of radius 30 m with a gradually increasing speed. The steering was actively controlled stay on the circle. The vehicle was started at 10 km/h, and every 20 seconds the speed was increased by 4km/h until loss of control or maximum speed. The test was performed in both directions (CW and CCW).

ASSUMPTIONS

- This test was performed on pavement.

RESULTS

The following plot shows the result from the vehicle turning CCW.

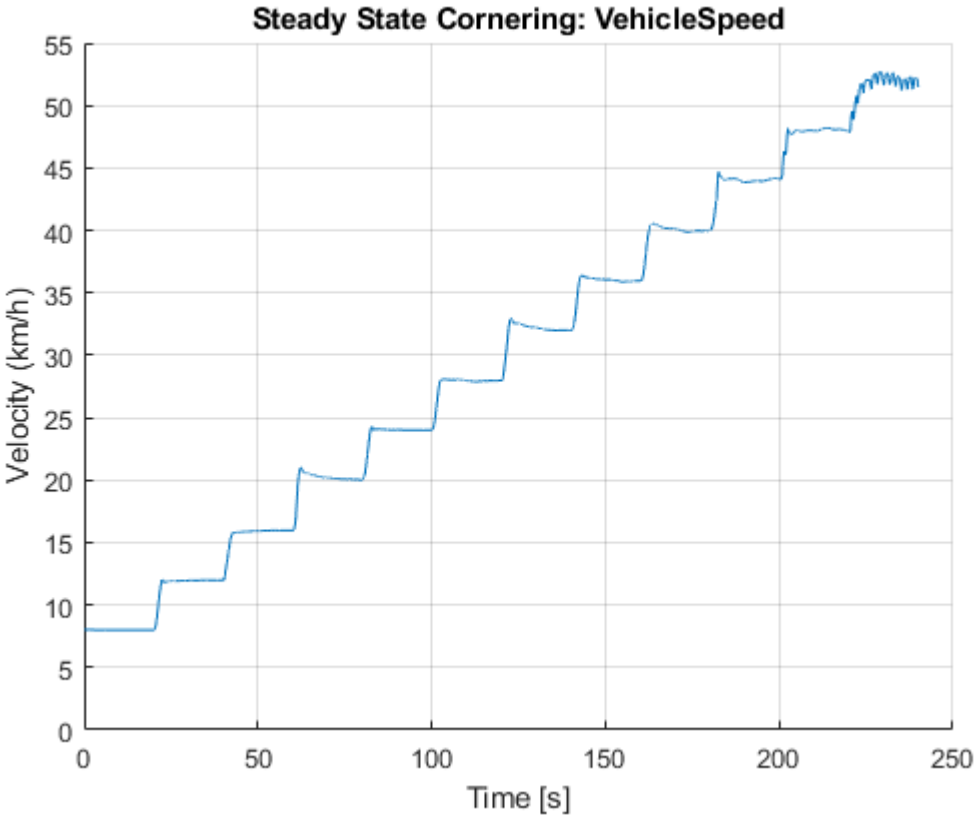

Figure 4: Vehicle speed for steady state turning CCW

Since the actual vehicle test was not run with the same procedure of incremental speed increases, direct plots of data compared to time are not comparable. Instead, a useful plot is to compare how the steering systems must be controlled at a given lateral acceleration, as in Figure 5.

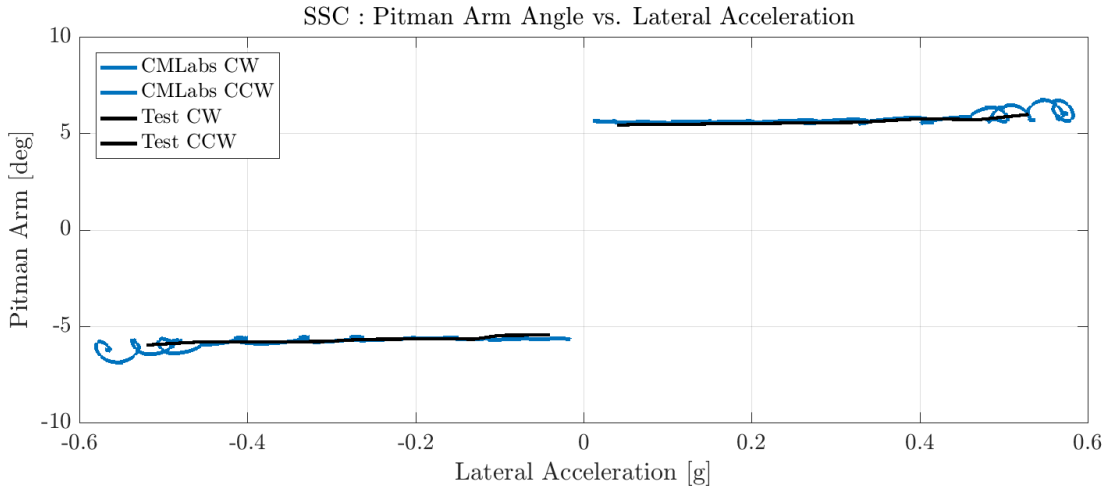

Figure 5: Chassis roll angle for steady state turning left

COMMENTS AND CONCLUSIONS

The results show a very close correlation between simulation and test results, indicating the steering and suspension system models very accurately reproduce the real systems.

Chapter 6 – Tests 4 and 5: Double Lane Change

In this test, the vehicle was driven through a double lane change manoeuvre as described in procedure AVTP 03-160 W.

Tests were performed two different ways. For calibration, a test was performed where the steering inputs of the simulation were directly driven by the measured inputs from a test run with the real vehicle. This allows the various vehicle measurements, such as lateral acceleration and body roll, to be compared between the simulation and real vehicle test. This test was only performed on pavement at 49 km/h, since that was the condition of the real vehicle test.

Tests were also performed to maximize the speed of the vehicle through the course. In this case, the path through the course was optimized in the simulation for maximum speed, and a driver model was used to follow the path. These simulation results cannot be directly compared to test results, since the vehicle was never driven at maximum speed through the course due to safety concerns. These tests were performed on pavement and Compacted Gravel in both directions; that is, first moving right then left (RtL) and left then right (LtR).

ASSUMPTIONS

- This test was performed on pavement and gravel (Compacted Gravel).

RESULTS

The test performed by playing back the real vehicle's steering inputs can be seen in Figure 6.

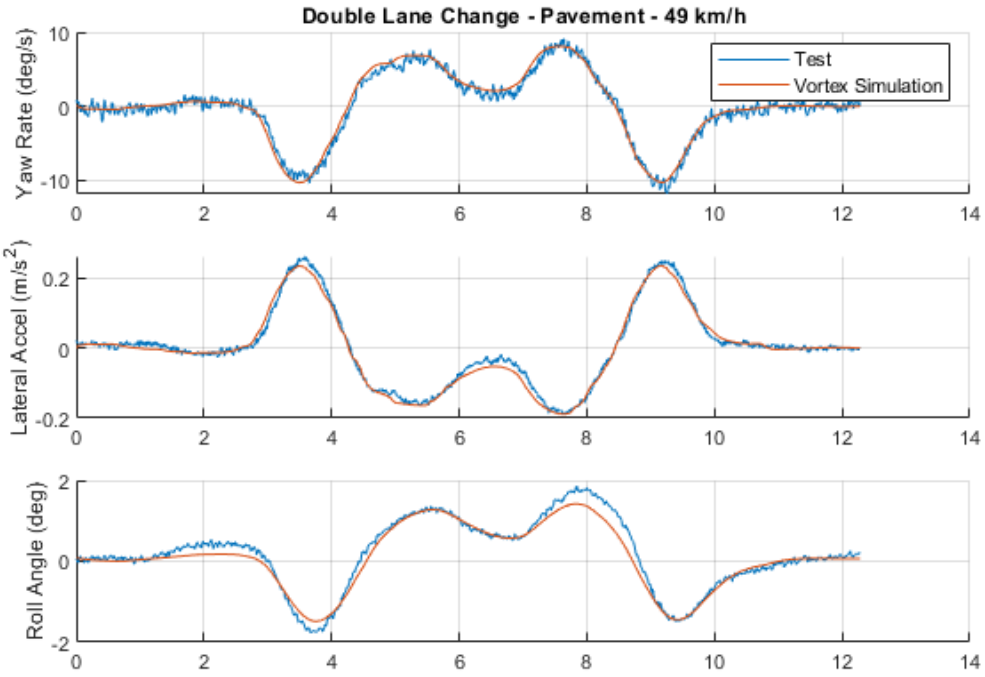

Figure 6: Yaw rate, Lateral acceleration and roll angle for vehicle on pavement at 49 km/h compared between CML simulation and KRC test

While the simulations that were optimized for speed do not have equivalent test results to compare to, the maximum speeds achieved can be seen in Table 5.

Table 5: Maximum speeds achieved for double-lane change simulation

Ground Type	Right then Left (km/h)	Left then Right (km/h)
Pavement	80	80
Compacted Gravel	65	65

COMMENTS AND CONCLUSIONS

Figure 6 shows a very close correlation between simulation and test results, indicating a highly accurate model of the steering and suspension systems in the vehicle model. The maximum speeds in Table 5 cannot be validated to vehicle tests, but seem reasonable.

Chapter 7 – Test 6: Side Slope Manoeuvre

In this test, the vehicle was driven across a 30% grade gravel side slope, and manoeuvred around an obstacle, represented by a pylon 3 meters below starting path, as seen in Figure 1.

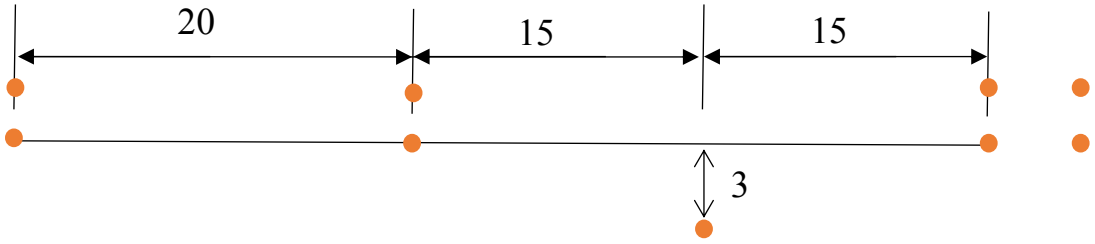

Figure 7: Side slope course

The test is performed solely to determine whether the vehicle can safely carry out the manoeuvre, and no required speed is specified.

ASSUMPTIONS

- This test was performed on gravel (Compacted Crushed Rock).

RESULTS

The path of the simulated vehicle traversing the obstacle can be seen in Figure 8.

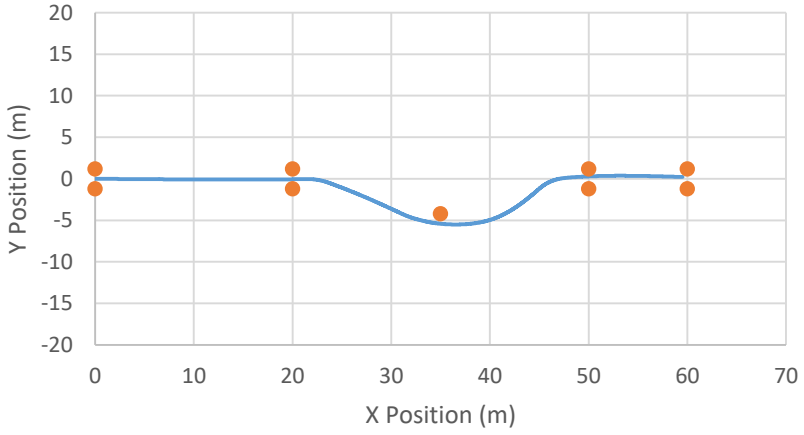

Figure 8: Path of vehicle around obstacle

COMMENTS AND CONCLUSIONS

In the simulation, the vehicle was able to safely traverse the course around the obstacle.

Chapter 8 – Test 7: Longitudinal Grade - Pavement

In this test, the vehicle attempted to climb a 60% paved ramp. The sole purpose is to determine if the vehicle can climb the ramp.

ASSUMPTIONS

- This test was performed on pavement.

RESULTS

The simulated vehicle was able to climb the ramp, which matches the real vehicle test, which was also able to climb the ramp.

COMMENTS AND CONCLUSIONS

The simulation correctly predicted that the vehicle can climb a 60% paved grade.

Chapter 9 – Test 8: Longitudinal Grade - Sand

In this test, the vehicle attempted to climb a gravel ramp of gradually increasing grade, from 0 to 30%. The purpose is to determine if the vehicle can climb the ramp.

ASSUMPTIONS

- This test was performed on 2NS sand.
- The simulation was performed using a simulated triangle mesh of the ramp measured from LIDAR scans of the real ramp, as seen in Figure 9.

Figure 9: Simulation sand ramp

RESULTS

The plot in Figure 10 shows the amount of wheel slip related to the slope of the ramp. The ramp slope has not been precisely measured, so the slope is estimated from the instantaneous pitch angle of vehicle.

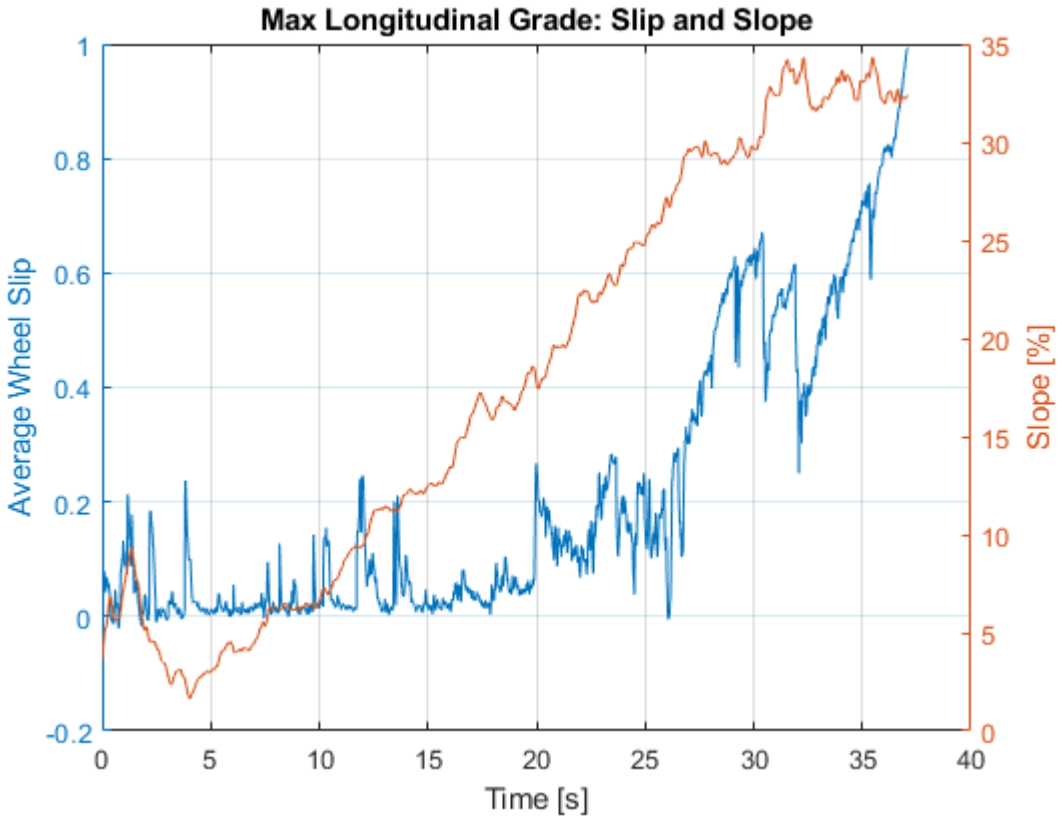

Figure 10: Wheel slip and slope of sand slope climb

This shows a maximum sand climbing capability in 2NS sand of about 33%, which is higher than the actual test capability of 18.5%.

COMMENTS AND CONCLUSIONS

The simulation significantly overestimated the climbing ability of the vehicle on 2NS sand, predicting a maximum slope of about 33%, while the real vehicle could only climb to about 18.5%. It was found that for several soil types, simulated results deviated significantly from real vehicle tests, as will be seen in Tests 16 – 18 Drawbar Pull. This was discussed and investigated in detail throughout the calibration and verification process, and no solid conclusions were reached. This should be further investigated.

Chapter 10 – Tests 9 – 12: Half-Rounds

In this test, the vehicle is driven at various speeds of a half-round obstacles, as seen in Figure 11.

Figure 11: Half-round bump

The vertical acceleration at the driver's seat base is measured in order to determine the maximum speed the vehicle can travel over the obstacle without exceeding 2.5 G of acceleration.

The test is performed on four different sized obstacles: 4, 8, 10, and 12-inch height.

ASSUMPTIONS

- This test was performed on pavement.
- Acceleration results are passed through a 4-pole, 30Hz Butterworth filter.

RESULTS

The following two plots show the seat acceleration and strut length for a single test: the 10-inch half-round at 28 km/h. This compares the actual measurements between the CML simulation and KRC test.

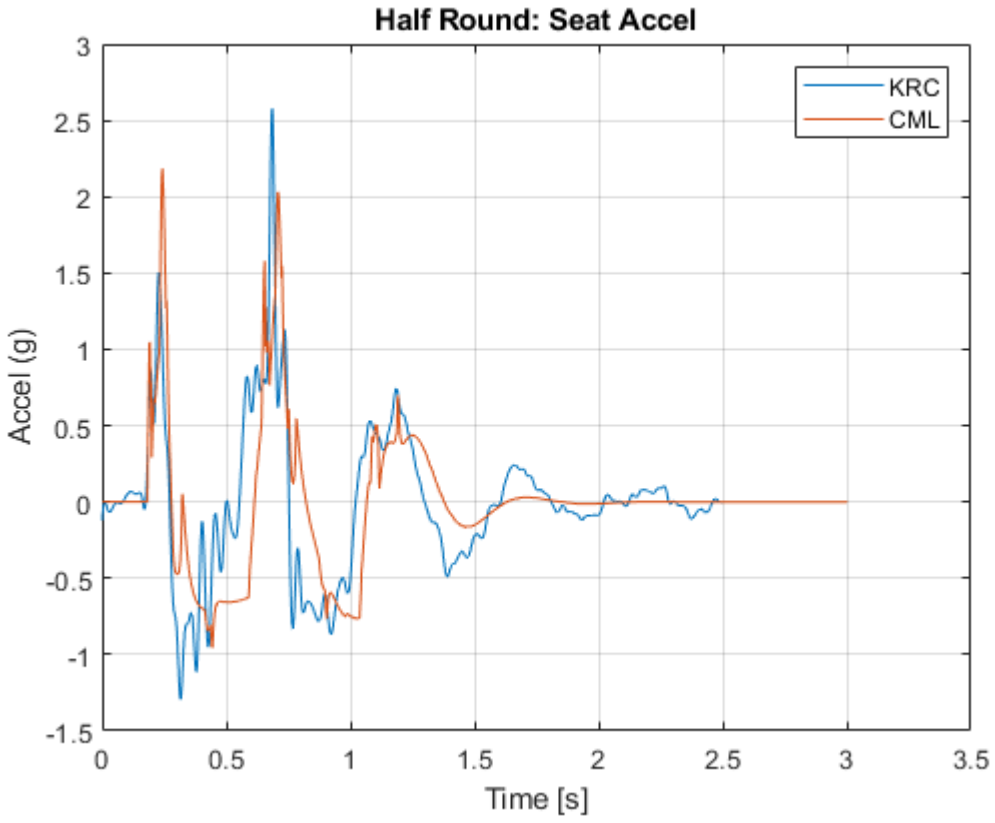

Figure 12: Seat base acceleration of 10-inch half-round at 28 km/h

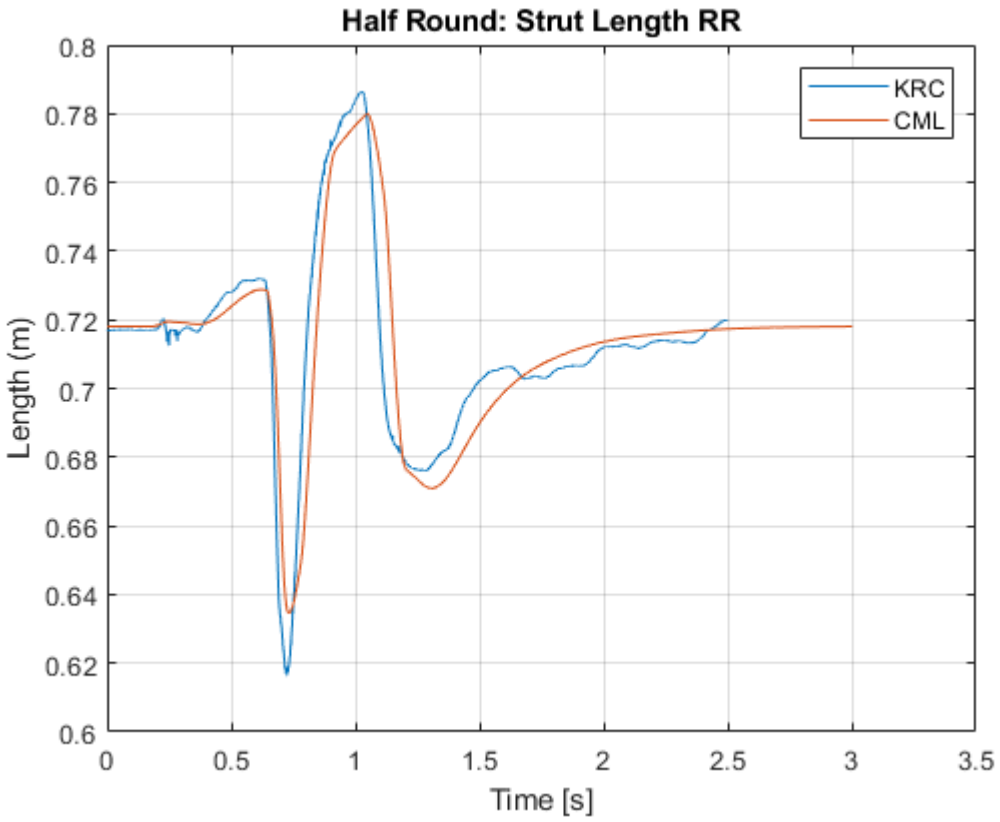

Figure 13: Right rear strut length of 10-inch half-round at 28 km/h

The ultimate goal of the test is to compare the maximum speed the vehicle can travel over the obstacles before reaching 2.5 G of vertical acceleration at the driver's seat. The comparison between CML simulation and KRC test results can be seen in Figure 14.

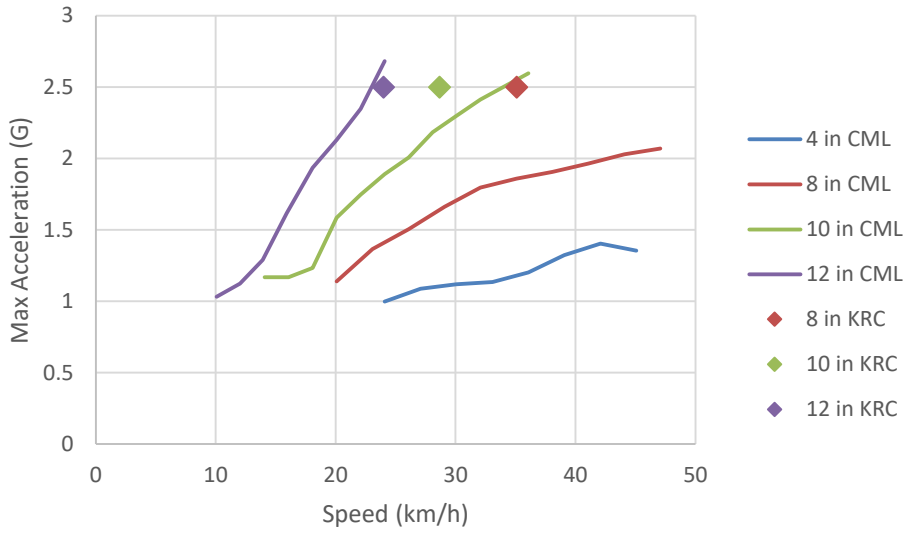

Figure 14: Maximum acceleration when hitting an obstacle at the given speed for four half-round sizes. Note that no speed results in 2.5 G for the 4-inch obstacle for both simulation and test results.

COMMENTS AND CONCLUSIONS

The plot of strut length shows the behaviour of the vehicle suspension is very similar to the real vehicle. However, the actual acceleration peaks vary significantly for the smaller half-round obstacles.

This test is highly sensitive to many parameters in the simulation and real test, such as sensor placement and mounting, chassis rigidity (which is not measured or simulated), and filtering of acceleration data. This compounded by the fact that the test is based on a peak acceleration value, when acceleration signals are notoriously noisy.

This means that large deviation can be expected in the maximum measured accelerations.

Instead, CML primarily focussed on calibration of the suspension strut behaviour, which seems to be a much cleaner, more reliable measurement of suspension behaviour. In order to achieve good behaviour, the frequency-selective damper model was significantly modified from the provided model, which could indicate that the performance of the damper has changed in the years since the damper was installed and tested.

Chapter 11 – Tests 13 – 15: Steps and V-Ditch Obstacles

In this test, the vehicle is driven slowly over steps of various heights (12, 18 and 24 inches) or a v-ditch to determine if it can cross. The obstacle is considered crossed if the vehicle can pass with minimal or no interference with the body of the vehicle.

ASSUMPTIONS

- This test was performed on pavement.
- The tests are performed slowly enough that dynamic effects are not important.

RESULTS

Figure 15 shows that the vehicle can cross the 12-inch step with no interference.

Figure 15: Vehicle crossing 12-inch step

However, the body of the vehicle would hit the 18-inch step, as seen in Figure 16. A step of 24 inches would clearly also cause interference.

Figure 16: Vehicle body would touch 18-inch step (orange circle)

The vehicle is able to cross the v-ditch, as in Figure 17, though the front tow hook is very close to contacting the ground.

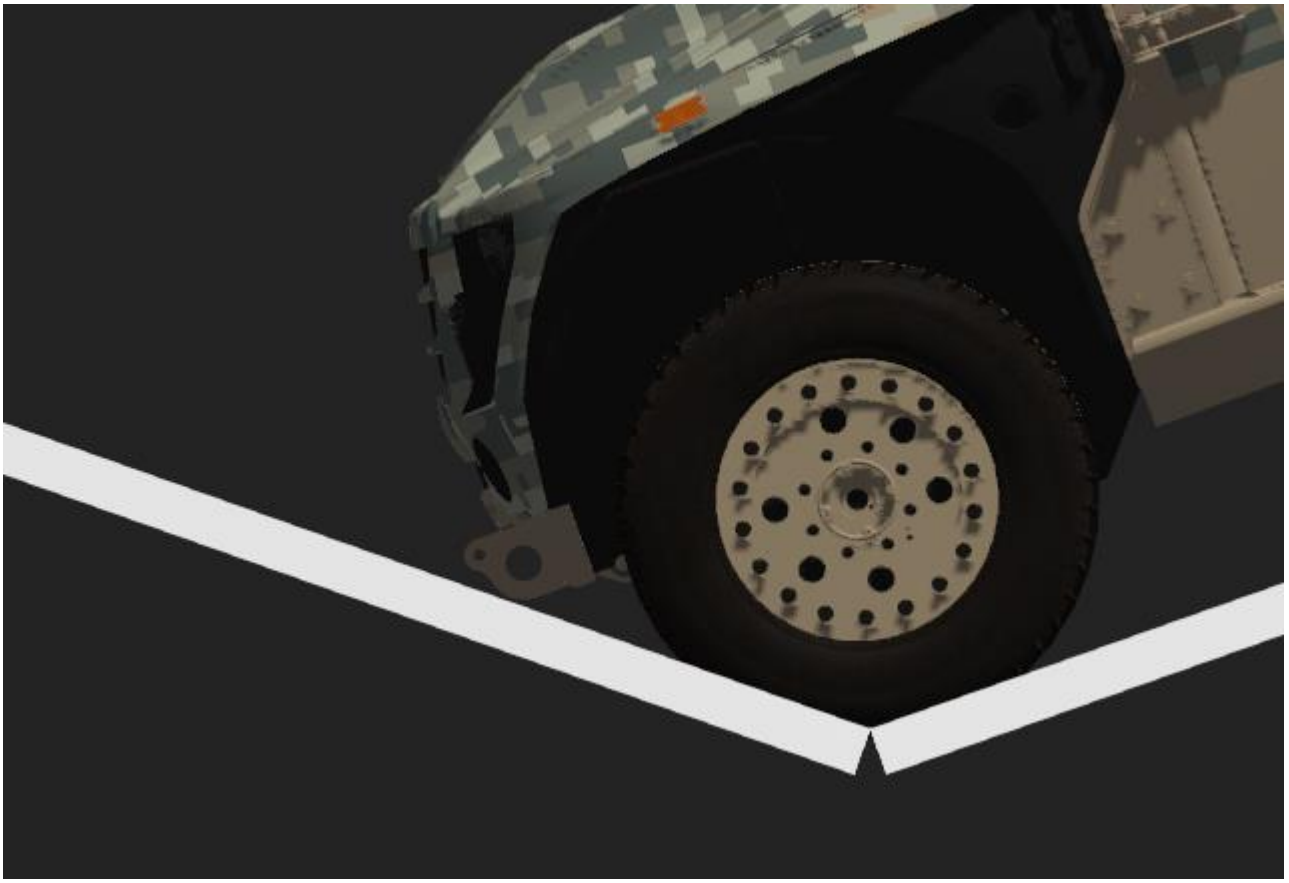

Figure 17: Vehicle crossing v-ditch

A summary of the results and comparison to KRC tests can be seen below.

Table 6: Obstacle Crossing

Obstacle	CML Simulation	KRC Test
12-inch Step	Go	Go
18-inch Step	No-Go	No-Go
24-inch Step	No-Go	No-Go
V-Ditch	Go	Go

COMMENTS AND CONCLUSIONS

Based on the results, the simulation is able to correctly predict the vehicle behaviour for all four obstacles, though in some cases, a difference of a few millimetres could change the results. This indicates that the simulation can very accurately capture the geometry of the real vehicle.

Chapter 12 – Tests 16 – 18: Drawbar Pull

In this test, the vehicle is over an area of soft soil. A towed vehicle is connected with a cable, and the tension in the cable (drawbar pull) is gradually increased until the test vehicle is immobilized.

ASSUMPTIONS

- This test was performed on pavement.
- The tests are performed slowly enough that dynamic effects are not important.

RESULTS

The following plots show the drawbar pull coefficient (drawbar pull force divided by total vehicle weight) plotted as a function of slip percentage ([wheel spindle speed – actual vehicle speed] / wheel spindle speed).

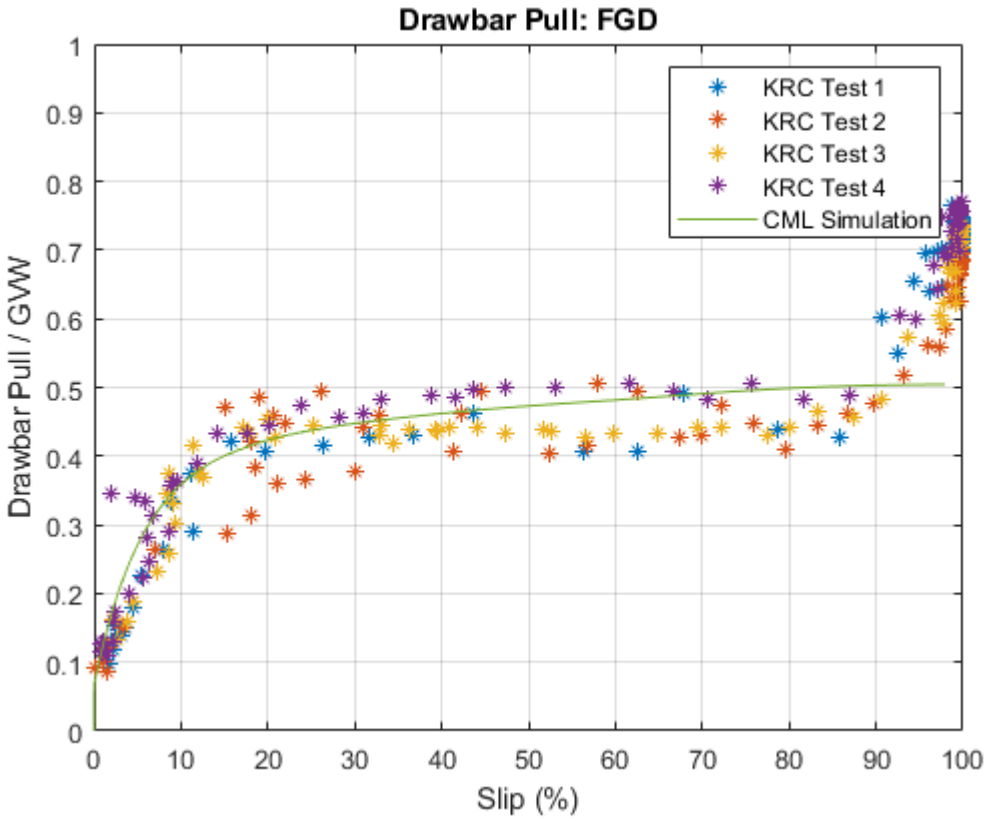

Figure 18: Drawbar pull on FGD

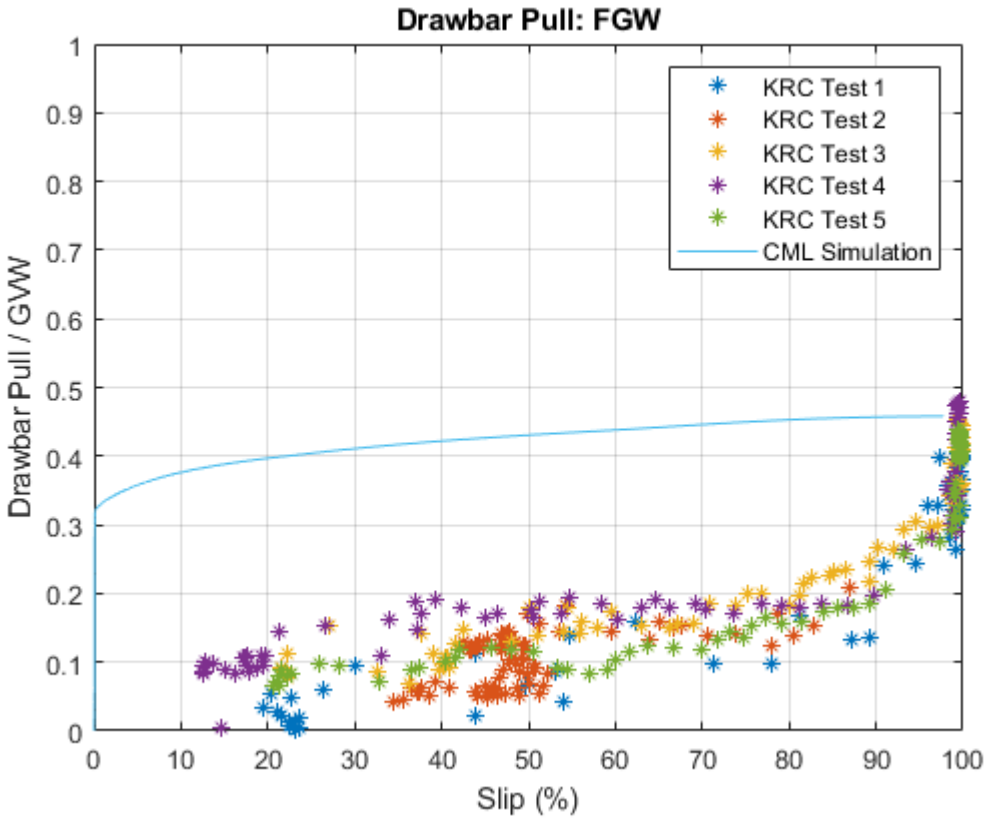

Figure 19: Drawbar pull on FGW

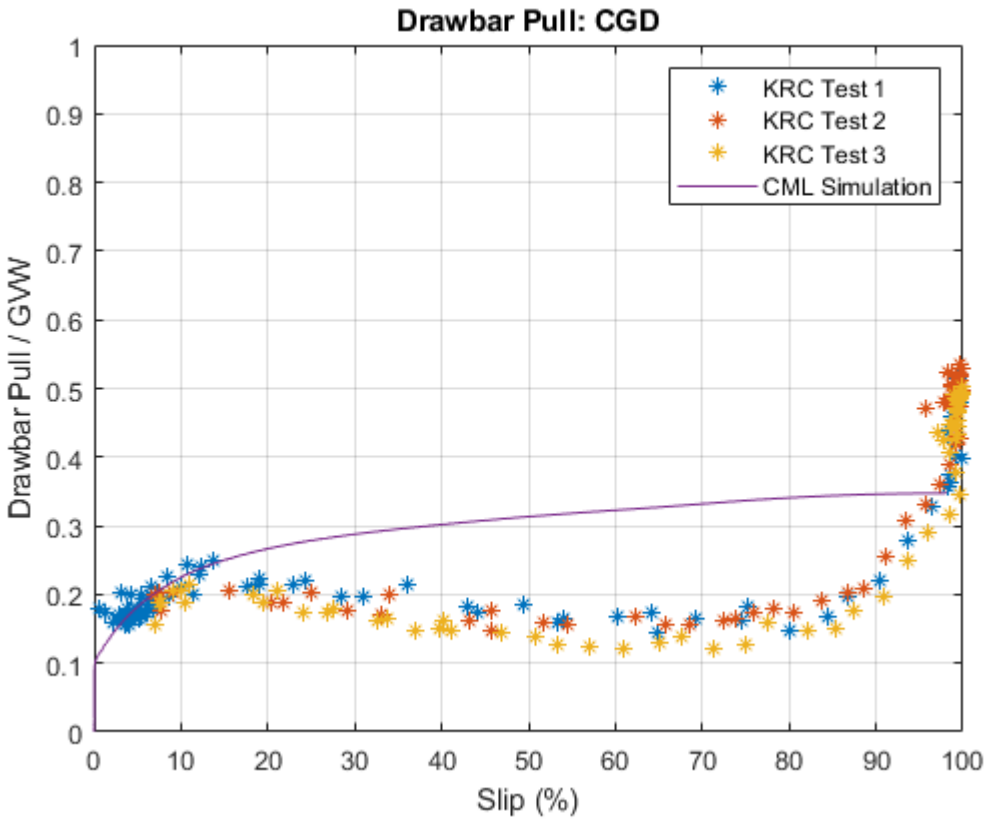

Figure 20: Drawbar pull on CGD

COMMENTS AND CONCLUSIONS

Based on these results, it seems that certain soil types are modelled well, others are not. The simulation results on FGD soil seemed to correlate very well to test results. Simulation of CGD were accurate up to about 15% slip, but deviated at higher slip levels. Simulation of FGW significantly overpredicted traction.

This is a significant issue that is related to similar overpredictions in soil performance in the sand climbing event. This has been discussed in detail throughout the calibration and verification process, and should be further investigated.

Chapter 13 – Tests 20 – 31: Ride Quality

The ride quality test is a standard test to determine how much power is transmitted to the driver over a rough course (US Army TOP 1-1-014). The vehicle is driven over several courses with bumps of an average RMS (root-mean-squared) height, varying from 1 to 4 inches, and the vertical acceleration of the vehicle is used estimate the power absorbed by the driver. A continuous power over 6 Watts is considered tiring and unacceptable for a driver.

ASSUMPTIONS

- This test was performed on three different soil types as described in Table 2: Fine grain soil, dry (FGD), fine grain soil, wet (FGW) and coarse grain soil (CGS).
- Absorbed power was calculated from vertical acceleration at the seat base. It does not include lateral and longitudinal accelerations, and the seat base is assumed to be rigidly connected to the chassis.

RESULTS

The following plot shows the simulation results for what speed results in than 6 W of power on the driver, compared to the actual vehicle speed when 6 W was measured for five different RMS courses: 1, 1.5, 2, 3, and 4 inches. These are symmetric tests, where both wheels are driving on the same profile.

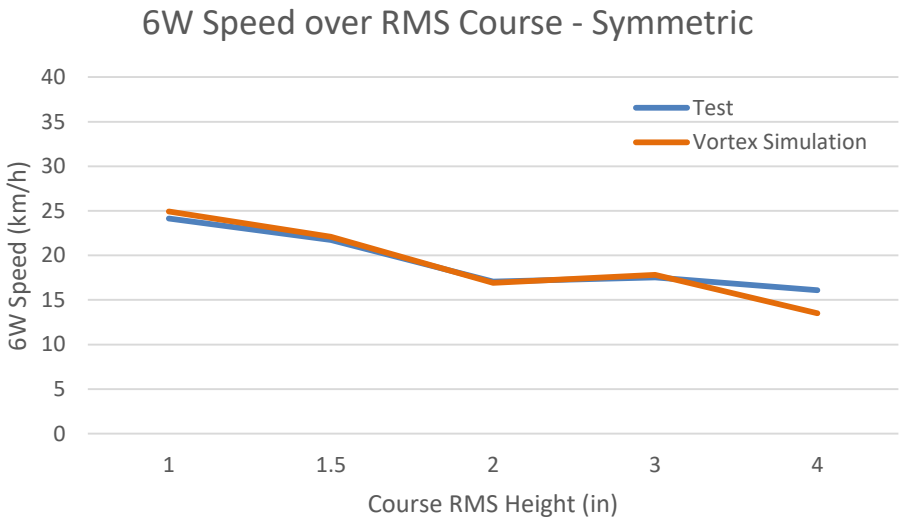

Figure 21 Symmetric course 6 W speeds

Asymmetric tests were also performed, where each side of the vehicle (right and left) are on different profiles. In this case, only two cases were considered, 1 and 1.5 inch, and 1.5 and 2 inch.

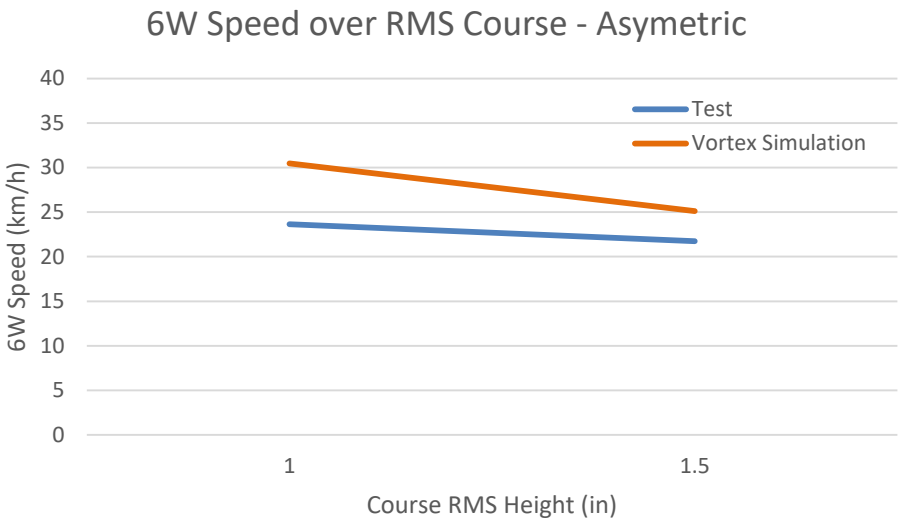

Figure 22 Asymmetric course 6 W speeds

COMMENTS AND CONCLUSIONS

The symmetric results show a very close correlation between simulation and test results. The asymmetric results have some amount of deviation, but are still within a reasonable range of accuracy.

Chapter 14 – Test 32: Mobility Traverse

In this event, the vehicle is driven through a contiguous 5 km route across KRC's testing grounds, as seen below.

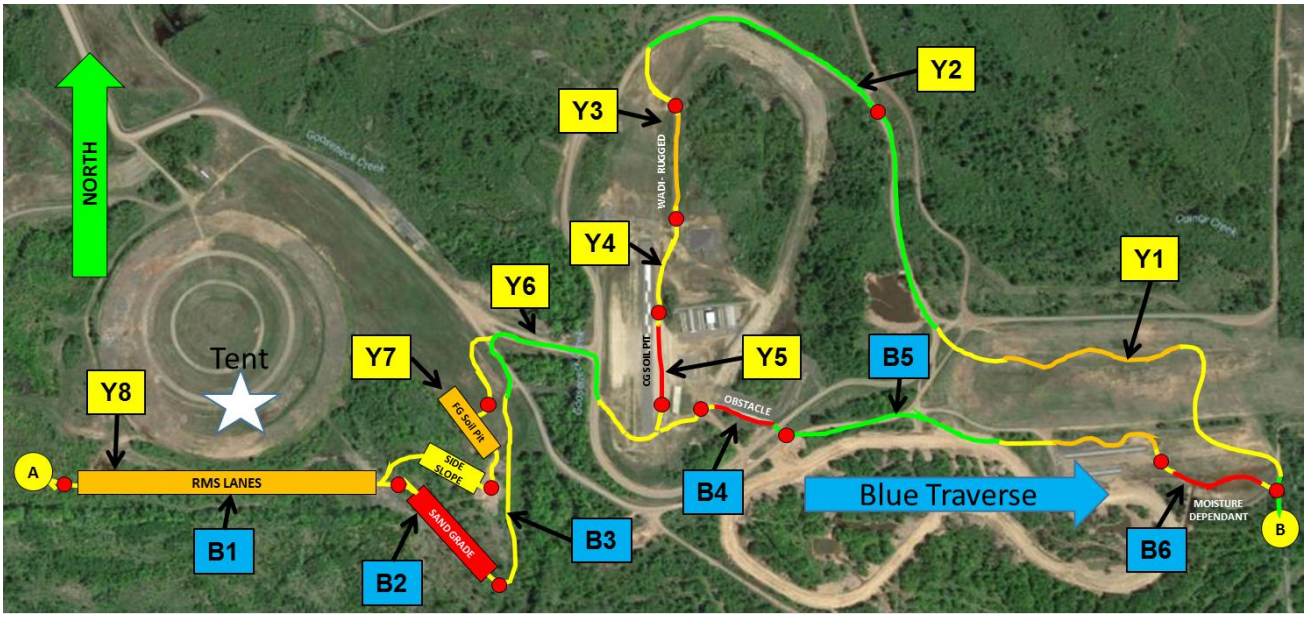

Figure 23 Mobility traverse route across KRC

While the entire traverse route is a complete loop, it is divided into individual sections to allow the driver to change vehicle settings (locked differentials, low/high range) and to provide smaller pieces that can more easily be compared. CM Labs was assigned six traverse sections to simulate and analyse: Y3, Y5, Y8, B3, B4, B5.

The terrain for the traverse was modelled in the simulation environment based on triangle information from LIDAR scans of the KRC testing grounds. While Vortex Studio includes support for many standard triangle formats, a custom converter was developed to translate the provided LandXML files into .fbx format that could be imported.

In the process of importing and testing terrains from KRC, several features were found that seemed to be unrealistic. In most cases, this could be traced to vegetation that was erroneously appearing to the LIDAR scanner as spikes in the ground. KRC went through several iterations of the terrain, manually cleaning and smoothing certain parts of the terrain.

CM Labs did not modify any terrain geometry from what was provided by KRC. However, some of the features of the terrain, such as thin triangles, very small triangles, or vertical triangles, could cause problems with Vortex Studio's contact detection. Therefore, a small amount of filtering (a least-squares plane was fit to an area the size of the wheel contact patch) was added to the contact detection algorithm to avoid these problems.

Terrain properties are taken from actual in-situ measurements, as summarized in Table 1 and Table 2. Since each traverse could drive over many different terrain types, a system was developed to load a provided GeoTIFF file into Vortex Studio, and query the terrain type from the file for the location of the vehicle.

Control of the vehicle through the tests was carried out with a path-following driver model. A GPS path was provided by KRC for the actual vehicle test, and the software developers were asked to determine the maximum possible speed.

ASSUMPTIONS

- Speed of the vehicle was optimized to be as high as possible, without losing control.

RESULTS

The following plot shows the simulation and test speeds for the six mobility traverse sections.

Figure 24 Simulated and test speeds for traverse section Y3

Figure 25 Simulated and test speeds for traverse section Y5

Figure 26 Simulated and test speeds for traverse section Y8

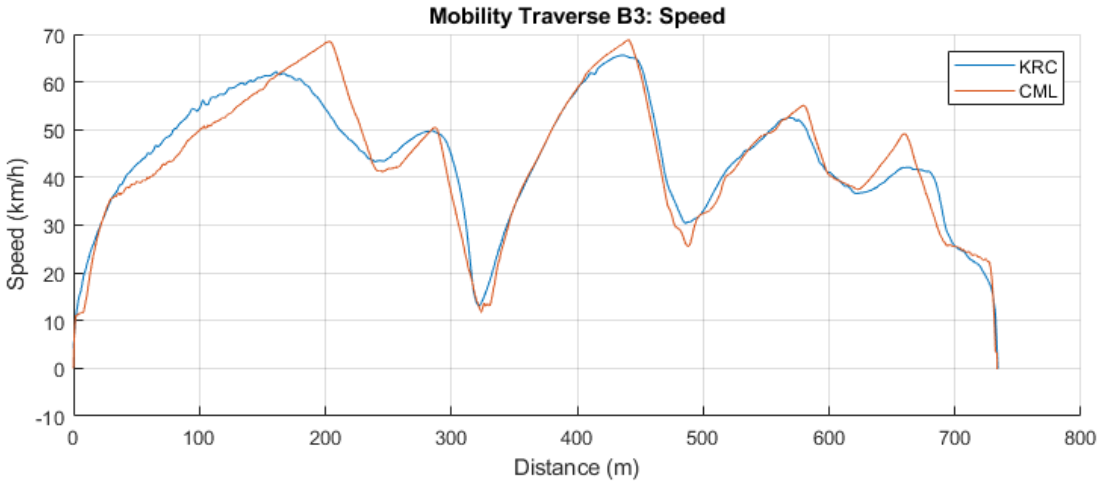

Figure 27 Simulated and test speeds for traverse section B3

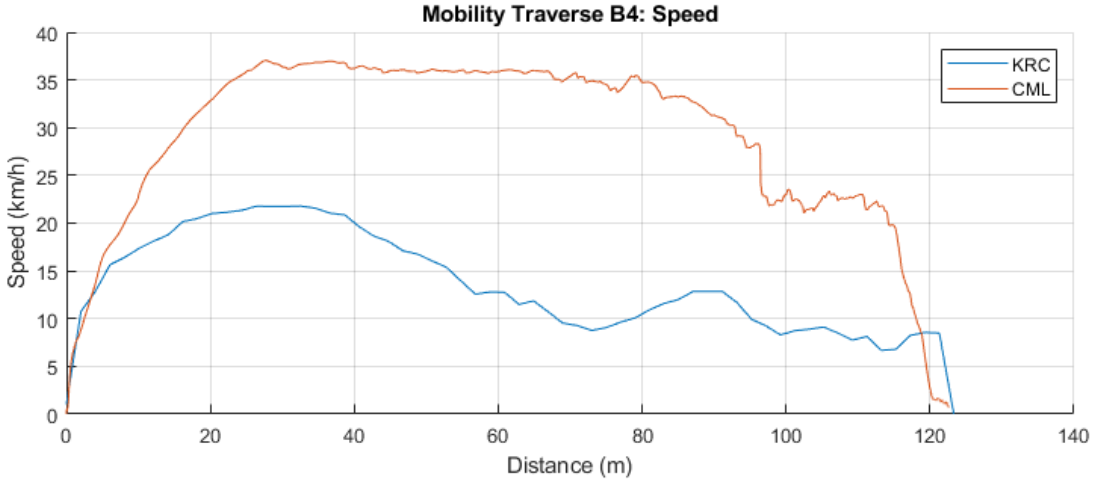

Figure 28 Simulated and test speeds for traverse section B4

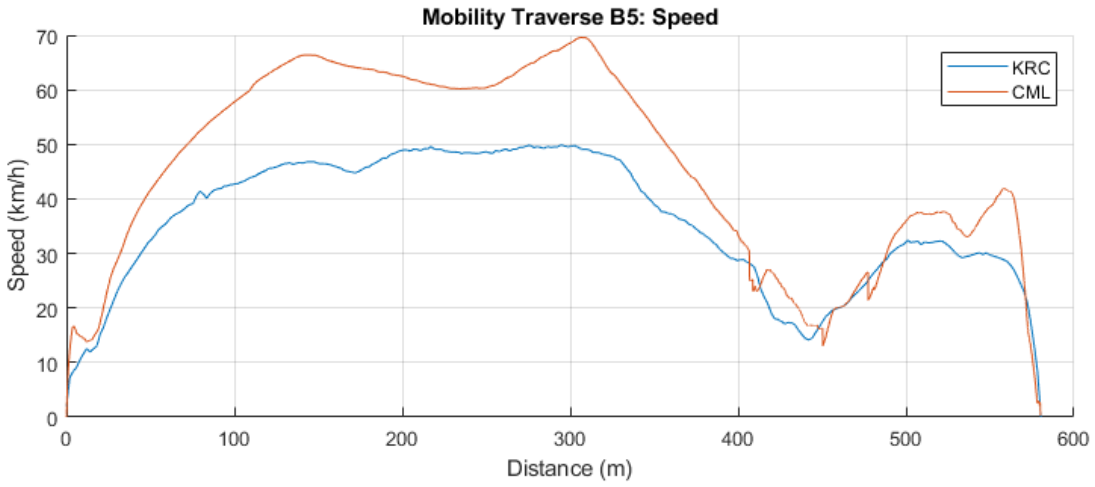

Figure 29 Simulated and test speeds for traverse section B5

COMMENTS AND CONCLUSIONS

In some of the sections, such as Y5, Y8, B3 and B5, simulated speed results are very similar to test results. In these cases, the speed is primarily limited by acceleration, braking, and traction. These are cases where the behaviour of the driver model closely matches the actual test driver, and since the vehicle model has already been validated to be accurate in acceleration and handling, the traverse simulation can accurately predict driver behaviour.

There are some sections where simulation results significantly differ from test results, such as Y3 (wadi crossing) and B4 (OEF trail). Both of these sections are extremely rough and treacherous, and the test driver is reducing speed to avoid damaging the vehicle. Since the simulated driver model was not designed with these concerns, it is willing to drive faster than the test driver.

There are also parts of other sections, such as the beginning of Y8, where the simulated driver also drove faster than the test driver. In this case, there is a dangerous bridge crossing that the real driver was cautious about, whereas the simulated driver had no such concerns, and drove faster.

The mobility traverse results indicate the simulation is able to accurately predict vehicle behaviour. But there are cases where the driver model was programmed based on different criteria than a real driver would have used to make decisions.

Chapter 15 – Go / NoGo Maps

In addition to the testing and calibration events, a set of Go / NoGo maps was also generated for the KRC testing grounds. These maps indicate whether the vehicle is predicted to be able to pass (and at what speed) a homogeneous terrain unit with defined properties for soil parameters and slope. Each of these units is then compiled into a complete map of the KRC test site.

Rather than run the millions of trials needed to compile a statistically representative sample of parameters for each terrain unit, CM Labs worked with RAMDO Solutions to generate the maps. CM Labs carried out enough simulation runs with a variety of parameters, which RAMDO then used to build a surrogate model of the vehicle performance. That surrogate model was then used by RAMDO to quickly simulate many conditions, and compile a map.

ASSUMPTIONS

- The test was performed using a specially selected set of soft soil parameters from RAMDO.
- The test was run by driving the vehicle at a slowly increasing slope until it was immobile.

RESULTS

The following figures show the maps generated by RAMDO, based on simulation results from CM Labs. The legend of speed corresponding to color is shown here.

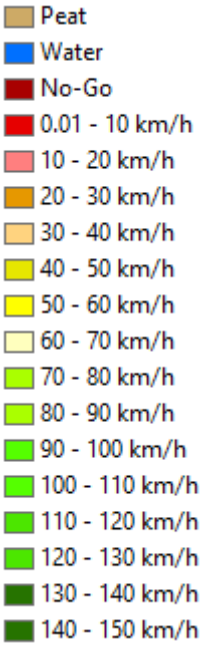

Figure 30 Speed made good legend

The first map show a deterministic map of speed made good, which is the estimated maximum speed of the vehicle using just the directly measured soil and slope parameters. If all measurements are perfect, this map should indicate an accurate prediction of speed.

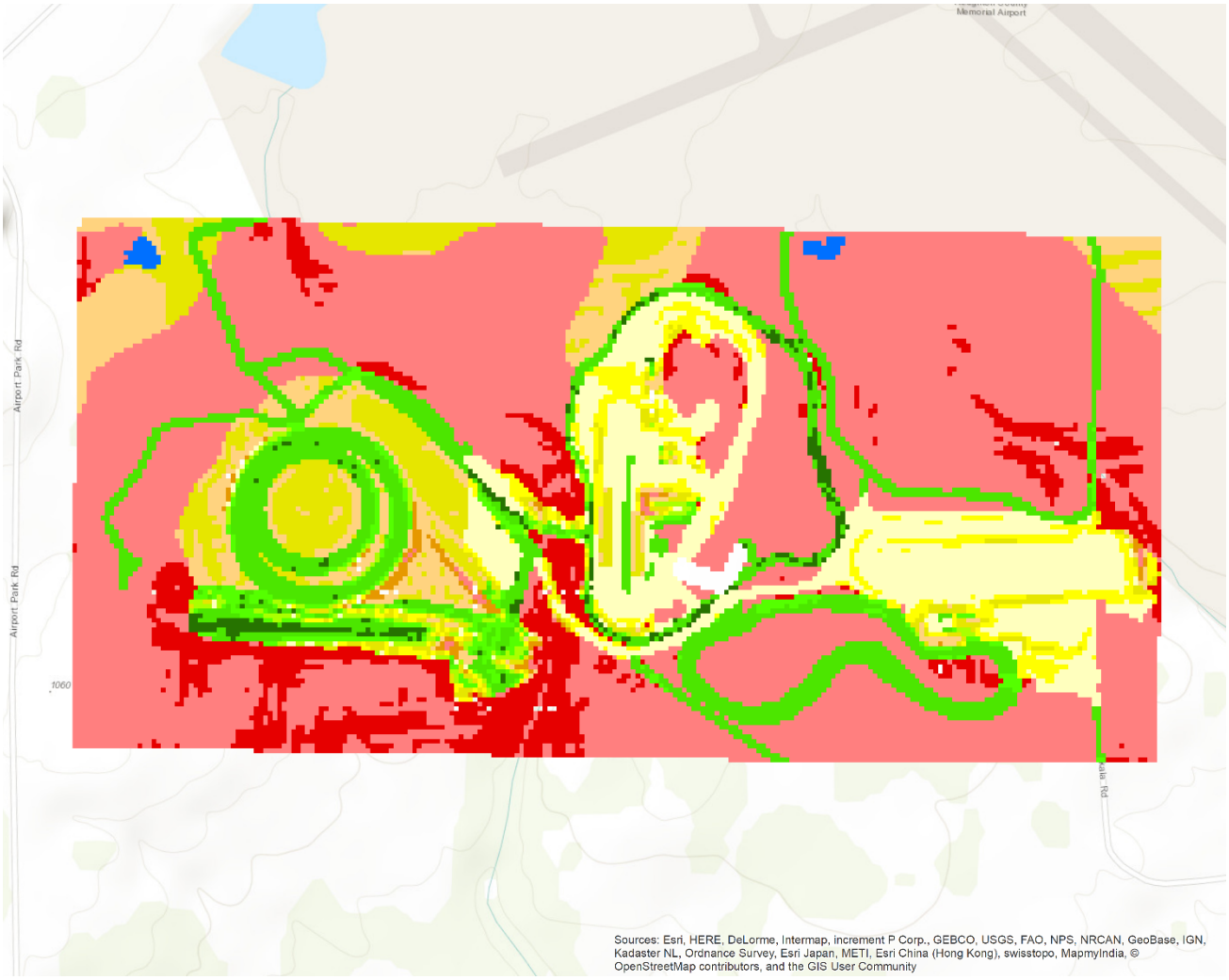

Figure 31 Deterministic speed made good

However, measurements are never perfect. The following maps show probabilistic speed made good, which use samples over a range of soil parameters to predict the probability that vehicle can actually traverse at the given speed.

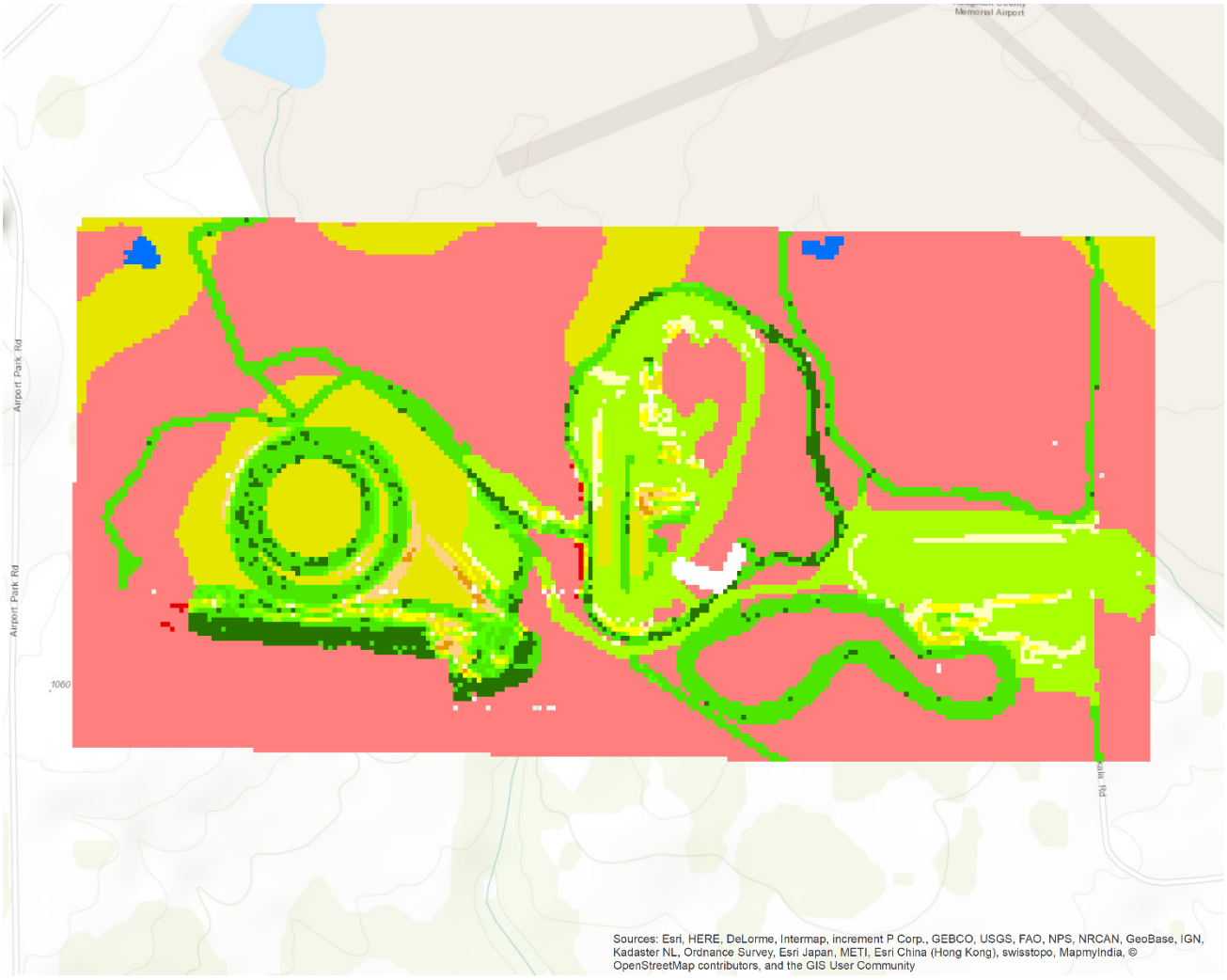

Figure 32 Speed made good 10% probability

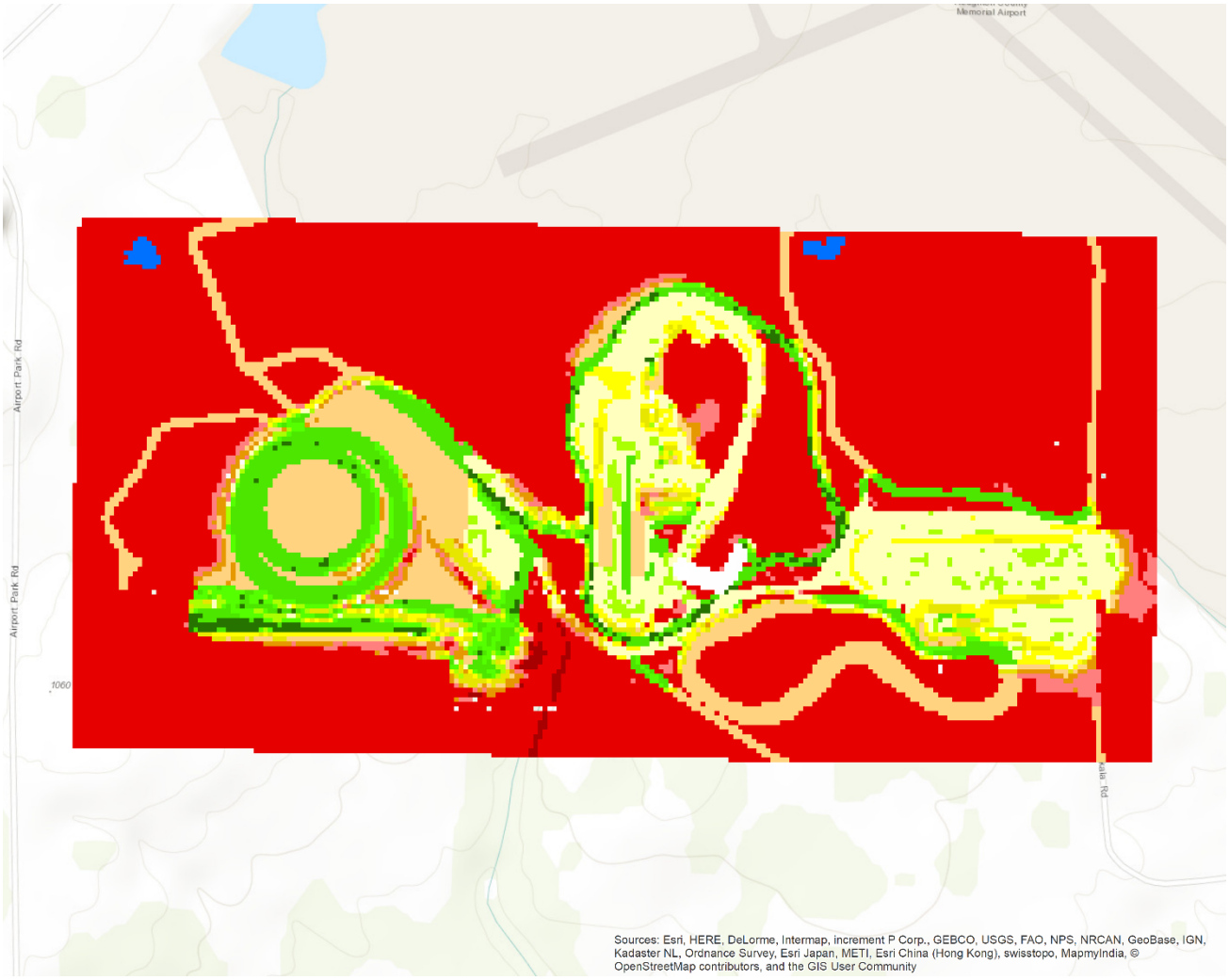

Figure 33 Speed made good 90% probability

COMMENTS AND CONCLUSIONS

The maps show a predicted speed achievable by the vehicle in the corresponding location on the KRC testing grounds. As expected, the speeds are lower when considering 90% probability than 10% probability. The deterministic map shows some relation to both probabilistic maps.

Chapter 16 – References

[1] Azimi, A. *Wheel-Soil Interaction Modelling for Rover Simulation and Analysis.* Ph.D. Thesis, McGill University, Department of Mechanical Engineering, Montréal, 2013.

[2] Azimi, A., Holz D., Kövecses, J., Angeles, J., Teichmann, M., A Multibody Dynamics Framework for Simulation of Rovers on Soft Terrain. *ASME Journal of Computational and Nonlinear Dynamics*, Vol. 10, No. 3, pp. 031004-1-12, 2015.

[3] Bekker, M.G. *Theory of Land Locomotion*. Ann Arbor, The University of Michigan Press, 1956.

[4] Bekker, M.G. *Off-the-road locomotion; research and development in terramechanics.* Ann Arbor, The University of Michigan Press, 1960.

[5] Z. Janosi and B. Hanamoto. *Analytical determination of drawbar pull as a function of slip for tracked vehicles in deformable soils*. In First Int. Conf. on Terrain-Vehicle Systems, Turin, Italy, 1961.

[6] Wong, J. Y. and Reece, A. R. Prediction of rigid wheel performance based on the analysis of soil-wheel stresses part I: Performance of driven rigid wheels. *J. Terramechanics*, 4(1):81–98, 1967a.

[7] Yoshida, K., Ishigami, G. (2004). Steering characteristics of a rigid wheel for exploration on loose soil. In *2004 IEEE/RSJ International Conference on Intelligent Robots and Systems (IROS)* (Vol. 4, pp. 3995-4000)